Nucleic Acids Research, 2002, Vol. 30 No. 21 **4643–4649**

A Cajal body-specific pseudouridylation guide RNA is composed of two box H/ACA snoRNA-like domains

Arnold M. Kiss[1,2], Beáta E. Jády[3], Xavier Darzacq[1], Céline Verheggen[3], Edouard Bertrand[3] and Tamás Kiss[1,2,*]

[1]Laboratoire de Biologie Moléculaire Eucaryote du CNRS, Université Paul Sabatier, 118 route de Narbonne, 31062 Toulouse Cedex, France, [2]Biological Research Center, Hungarian Academy of Sciences, Szeged, Hungary and [3]Institut de Génétique Moléculaire, Montpellier, France

Received July 17, 2002; Revised and Accepted September 9, 2002

DDBJ/EMBL/GenBank accession no. AF492209

ABSTRACT

Site-specific post-transcriptional conversion of uridines to pseudouridine in ribosomal RNAs and small nuclear RNAs (snRNAs) is directed by guide RNAs which possess the conserved box H and ACA sequence elements and fold into the consensus 'hairpin–hinge–hairpin–tail' secondary structure. Here, we describe an unusual mammalian pseudouridylation guide RNA, called U93, that is composed of two tandemly arranged box H/ACA RNA domains. The U93 RNA therefore carries two H and two ACA box motifs, all of which are essential for accumulation of the full-length RNA. The human U93 RNA accumulates in Cajal (coiled) bodies and it is predicted to function in pseudouridylation of the U2 spliceosomal snRNA. Our results lend further support to the notion that modification of the RNA polymerase II-transcribed spliceosomal snRNAs takes place in Cajal bodies.

INTRODUCTION

The nucleus contains a large number of small nuclear RNAs (snRNAs) which possess diverse cellular functions (1). The U1, U2, U4, U5 and U6 spliceosomal snRNAs play a pivotal role in the removal of intron regions from pre-mRNAs. The U7 snRNA directs 3′-end formation of histone mRNAs and the RNase P RNA functions in 5′-end processing of tRNAs. The U3, U8, U14, U22, snR30 and MRP small nucleolar RNAs (snoRNAs) are required for the production of mature ribosomal RNAs (rRNAs) (2). Besides RNA processing, snRNAs also function in the regulation of transcription elongation by RNA polymerase (pol) II (7SK RNA) (3,4) and in the synthesis of telomeric DNA repeats (telomerase RNA) (5). All snRNAs associate with specific proteins and form small nuclear or nucleolar ribonucleoprotein particles (snRNPs or snoRNPs) (1).

The nucleus also contains an enormous number of modification guide RNAs which direct the post-transcriptional synthesis of 2′-*O*-methylated nucleotides and pseudouridines in rRNAs, spliceosomal snRNAs and, most likely, other cellular RNAs (for recent reviews, see 6–11). The 2′-*O*-methylation guide RNAs possess the conserved box C (RUGAUGA) and D (CUGA) elements that are frequently tethered by a short 5′,3′-terminal stem (Fig. 1). The internal region of box C/D RNAs carries the C′ and D′ boxes which represent perfect or imperfect copies of the C and D boxes (12,13). The pseudouridylation guide RNAs are characterised by a consensus 'hairpin–hinge–hairpin–tail' structure and they carry the conserved H (ANANNA) and ACA box elements (14,15). The H box is located in the single-stranded hinge region after the 5′ hairpin. The ACA box is found in the 3′-terminal tail 3 nt before the end of the RNA. The box C/D 2′-*O*-methylation guide RNAs are associated with four RNP proteins, fibrillarin/Nop1p, Nop56p, Nop58p and 15.5kD/Snu13p, whereas the box H/ACA pseudouridylation guide RNAs specifically bind dyskerin/Cbf5p, Gar1p, Nhp2p and Nop10p (reviewed in 8–10). The guide RNAs provide scaffolding for the associated RNP proteins and select the target nucleotide by forming direct base-pairing interactions with the substrate RNA. In turn, the RNP proteins provide metabolic stability for the guide RNAs and catalyse the modification reactions. Most likely, the fibrillarin/Nop1p and dyskerin/Cbf5p RNP proteins perform the 2′-*O*-methyl transfer and the uridine to pseudouridine isomerisation reactions, respectively (16,17).

The modification guide RNAs accumulate either in the nucleolus or in the Cajal body and, accordingly, they are called snoRNAs or small Cajal body-specific RNAs (scaRNAs) (2,18). The two groups of modification guide RNAs possess different functions. The snoRNAs direct 2′-*O*-methylation and pseudouridylation of rRNAs (19–23) and the RNA pol III-transcribed U6 spliceosomal snRNA (24–26). The scaRNAs function in modification of the RNA pol II-specific U1, U2, U4 and U5 spliceosomal snRNAs (18,27).

*To whom correspondence should be addressed at Laboratoire de Biologie Moléculaire Eucaryote du CNRS, Université Paul Sabatier, 118 route de Narbonne, 31062 Toulouse Cedex, France. Tel: +33 5 61 33 59 91; Fax: +33 5 61 33 58 86; Email: tamas@ibcg.biotoul.fr

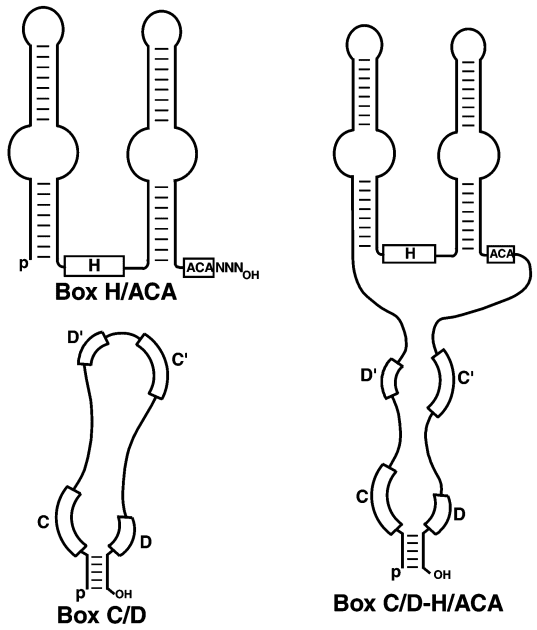

Figure 1. Classification of 2′-*O*-methylation and pseudouridylation guide RNAs. Schematic representation of the consensus two-dimensional structures of box C/D 2′-*O*-methylation, box H/ACA pseudouridylation and box C/D-H/ACA composite 2′-*O*-methylation and pseudouridylation guide RNAs. Positions of the conserved box elements are indicated.

The scaRNAs are frequently composed of a box C/D and a box H/ACA RNA-like domain (Fig. 1) and they can function both in 2′-*O*-methylation and pseudouridylation of snRNAs (18,27). Here, we describe a novel mammalian scaRNA, called the U93 RNA, that is predicted to function in pseudouridylation of the RNA pol II-specific U2 spliceosomal snRNA. Surprisingly, the human, mouse and cow U93 scaRNAs are composed of two tandemly repeated box H/ACA domains and therefore they contain two H and two ACA boxes which are all essential for accumulation of the full-length U93 RNA.

MATERIALS AND METHODS

General procedures

Unless stated otherwise, all techniques for manipulating DNA, RNA and oligonucleotides have been done as described by Sambrook *et al.* (28). The following oligonucleotides were used in this study: 1, ATGCCTCAGCTTCCTCT; 2, CAGACTTGCAGAAAAAGCA; 3, CAGTACTTAGTGTTCAACAGA; 4, ATAATCGATAATCTGTAGTCTTGGAGCCGC; 5, ATAGTCGACACTTGTGGCAGTACTTAGTG; 6, CAGCTTCCTCTGGAGTAGGGGGGTTCTGCAAGTCTGGTGT; 7, CAACAGTGACCAGAAACGGGCAGAGGAAAATTGCACA; 8, TCTATCCGCCAACAGTACCCCCCGCTTTGCAGTCGAGATA; 9, TATAGTCGACACTGGGGGCAGTACTTAGTGTTC; 10, GTGATAATGACTGGGCTATGTC; 11, AATACGACTCACTATAGGGGGCAGTACTTAGTGTTCAACAG; 12, AT*CTCGAGGGTACCACCAAT*CCTGTGCGGCTCCAT*A (amino-allyl-modified T residues are marked by asterisks).

Characterisation of human, mouse and cow U93 RNAs

A recombinant plasmid carrying a full-length cDNA of the human U93 scaRNA was identified during characterisation of a cDNA library of human HeLa snRNAs. Synthesis and cloning of cDNAs has been described (19). The 5′ terminus of U93 was confirmed by primer extension analysis using the terminally labelled oligonucleotide 1 as a primer. Partial cDNAs of the mouse and cow U93 scaRNAs were obtained by RT–PCR using oligonucleotides 2 and 3 as primers. The PCR-amplified fragments were cloned into the *Sma*I site of pBluescript (Stratagene) and subjected to sequence analyses. The 3′-terminal sequences of the mouse and cow U93 RNAs were determined by the oligoribonucleotide ligation–PCR amplification procedure (29), except that oligonucleotide 2 was used as a U93-specific upstream primer. The 5′-terminal sequences of mouse and cow U93 RNAs were determined by the RNA 5′-RACE procedure using oligonucleotide 1 as a primer.

Expression constructs

The coding region of the human U93 RNA gene was PCR amplified by using oligonucleotides 4 and 5 as primers and human genomic DNA as a template. The PCR product was digested with *Cla*I and *Sal*I and inserted into the *Cla*I and *Xho*I sites of the pCMV-globin expression vector (18), resulting in pCMV-globin-U93. Construction of derivatives of pCMV-globin-U93 carrying U93 genes with altered H1, H2 and ACA1 boxes was performed by the megaprimer amplification approach using pCMV-globin-H93 as a template (30). To obtain pCMV-globin-U93*H1* and pCMV-globin-U93*ACA1*, the 5′ half of the U93 gene was amplified with oligonucleotides 6 and 7 as mutagenic 3′ primers, respectively, and oligonucleotide 4 as a 5′-end-specific primer. The PCR products were used as megaprimers in the second amplification step in combination with a common 3′-end-specific primer (oligonucleotide 5). The amplified products were digested with *Cla*I and *Mlu*I and cloned into the *Cla*I and *Mlu*I sites of pCMV-globin. A similar strategy was used to generate pCMV-globin-U93*H2*, except that a megaprimer was generated with oligonucleotides 5 and 8 as 3′- and 5′-end-specific primers, respectively. In the second step of amplification, oligonucleotide 4 was used as a 5′-end-specific primer. Finally, amplification of the human U93 RNA gene with oligonucleotides 4 and 9 resulted in U93*ACA2*, which was inserted into the *Cla*I and *Xho*I sites of pCMV-globin, yielding pCMV-globin-U93*ACA2*. The identity of each expression construct was verified by sequence analyses. Construction of the coilin-Dsred2 expression vector has been described (31). Transfection of simian COS-7, human HeLa and mouse L929 cells has been described (18).

Immunoprecipitation, cell fractionation and RNA analysis

Immunoprecipitation of human snRNPs with anti-fibrillarin and anti-hGAR1 antibodies (kindly provided by Drs J. A. Steitz and W. Filipowicz, respectively) was performed as described (18). Fractionation of HeLa cells into nuclear, nucleoplasmic, nucleolar and cytoplasmic fractions was performed according to Tyc and Steitz (32). From COS-7 and HeLa cells and the nuclear, nucleolar, nucleoplasmic and

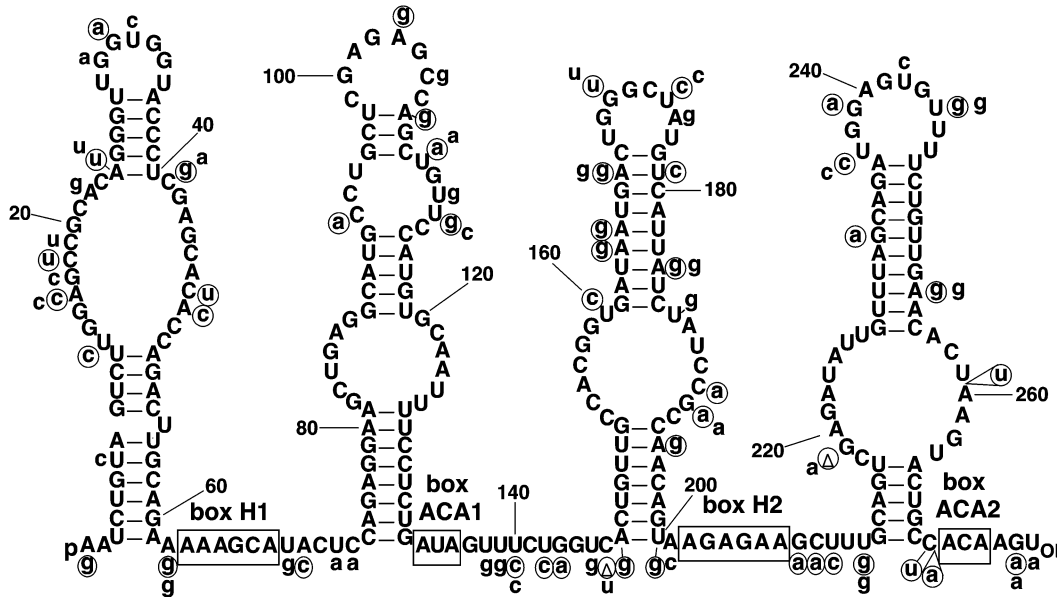

Figure 2. Primary and predicted two-dimensional structures of human, mouse and cow U93 box H/ACA-H/ACA RNAs. The nucleotide sequence of the human U93 RNA is in capitals. Lower case and circled lower case letters indicate changes in the mouse (*Mus musculus*) and cow (*Bos taurus*) U93 RNAs, respectively. Nucleotide deletions (Δ) and insertions (arrowheads) are also indicated. The putative box H (H1 and H2) and ACA (ACA1 and ACA2) sequences are boxed. Please note that nucleotides which might be involved in formation of putative pseudouridylation pockets are unfolded. The sequence of the human U93 RNAs is available in GenBank under the accession no. AF492209.

cytoplasmic fractions of HeLa cells, RNA was isolated by the guanidine thiocyanate/phenol–chloroform extraction procedure (33). RNase A/T1 protection was performed as described by Goodall *et al.* (33). For mapping of U93, U93*H1*, U93*ACA1*, U93*H2* and U93*ACA2* RNAs, sequence-specific RNA probes were synthesised by SP6 RNA pol using *Nde*I-digested pCMV-globin-U93, pCMV-globin-U93*H1*, pCMV-globin-U93*ACA1*, pCMV-globin-U93*H2* and pCMV-globin-U93*ACA2* plasmids as templates. Probes for U3, U4 and U19 snRNAs have been described (18). After synthesis, all probes were purified on a 6% sequencing gel.

In situ hybridisation

Fluorescent *in situ* hybridisation, image acquisition and processing has been described (18). To generate antisense RNA probe for the human U93 RNA, a fragment of the U93 gene from position 159 to position 269 was PCR-amplified with oligonucleotides 10 and 11 as primers. Utilisation of oligonucleotide 11 as a 3′-end-specific primer resulted in inclusion of the T7 RNA polymerase promoter into the amplified fragment. The resulting PCR product was used as a template for *in vitro* transcription by T7 RNA polymerase in the presence of 5-(3-aminoallyl) uridine 5′-triphosphate. Detection of the 5′-terminal box H/ACA domain of the U93 RNA was performed by using an oligonucleotide probe complementary to the human U93 RNA from position 13 to 44 (oligonucleotide 12). The modified RNA and oligonucleotide probes were labelled with FluoroLink™ Cy5-monofunctional dye (Amersham) according to the protocol of the laboratory of Dr Singer (http://singerlab.aecom.yu.edu). Human p80 coilin has been detected by polyclonal rabbit anti-coilin antibody (kindly provided by Dr A. Lamond) as it has been described (18).

RESULTS

Identification of a novel Gar1p-associated human box H/ACA RNA

During sequence analysis of a cDNA library of human HeLa snRNAs, we have identified a 275 nt long RNA that showed no significant sequence similarity to any known human RNA (Fig. 2). Northern analysis and RNase A/T1 protection experiments confirmed that the new RNA, called hereafter as U93, efficiently accumulates in HeLa cells (Figs 3 and 4; data not shown). The presence of an ACA triplet 3 nt before the 3′ terminus of the U93 RNA indicated that it might belong to the family of box H/ACA RNAs. Indeed, a monoclonal antibody directed against the human Gar1 protein, a component of box H/ACA RNPs, specifically precipitated the U93 RNA as well as the U19 box H/ACA snoRNA from a human HeLa cell extract (Fig. 3A). In contrast, an anti-fibrillarin antibody failed to precipitate both U93 and U19, but recognised the fibrillarin-associated U3 box C/D snoRNA. As expected, neither the anti-fibrillarin nor the anti-GAR1 antibody reacted with the U4 spliceosomal snRNP, demonstrating that the human U93 RNA specifically associates with the Gar1 snoRNP protein and it belongs to the family of box H/ACA RNAs.

Mammalian U93 snRNA is composed of two box H/ACA RNA-like domains

Computer modelling was used to generate a secondary structure for the human U93 RNA (34). In contrast to the consensus ‘hairpin–hinge–hairpin–tail’ structure of box H/ACA snoRNAs (Fig. 1), the computer-predicted structure of U93 is composed of four hairpins connected by three single-stranded hinge regions and terminated by a short tail (Fig. 2).

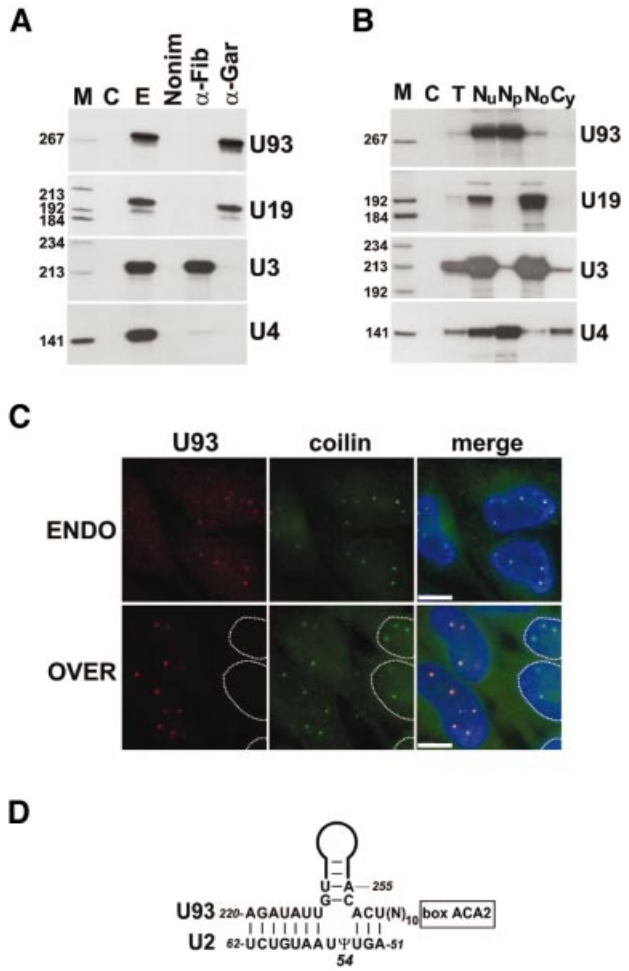

Figure 3. Characterisation of human U93 RNA. (**A**) Immunological characterisation of U93 RNP. RNAs recovered from the pellet of immunoprecipitation reactions performed with anti-hGAR1 (α-Gar), anti-fibrillarin (α-Fib) or a control non-immune serum (Nonim) from a human HeLa cell extract were mapped with sequence-specific antisense RNA probes indicated on the right. Lanes C and E show control mappings with RNAs obtained from *Escherichia coli* and HeLa cell extracts, respectively. Lane M, size marker (a mixture of *Hea*III- and *Taq*I-digested pBR322). (**B**) Cell fractionation. RNA isolated from HeLa cells (T), from the nuclear (Nu), nucleoplasmic (Np), nucleolar (No) and cytoplasmic (Cy) fractions of HeLa cells were mapped by sequence-specific antisense RNA probes as indicated on the right. (**C**) *In situ* localisation of U93 RNA. Human HeLa cells either transfected (bottom) or non-transfected (top) with the pCMV-globin-U93 expression construct (see Fig. 4A) were probed with a fluorescent RNA probe complementary to the human U93 RNA. Cajal bodies were detected by an antibody directed against human p80 coilin. Merged images show that the U93 RNA co-localises with p80 coilin both in transfected and non-transfected cells. The nuclei of non-transfected cells are highlighted by dotted lines. Under the exposure conditions shown, the endogenous U93 RNA remains invisible in non-transfected cells. (**D**) Potential base-pairing interaction of the human U93 and U2 RNAs. The 3′-terminal hairpin of U93 is schematically indicated. The U54 residue known to be pseudouridylated in vertebrate U2 snRNAs is indicated (Ψ).

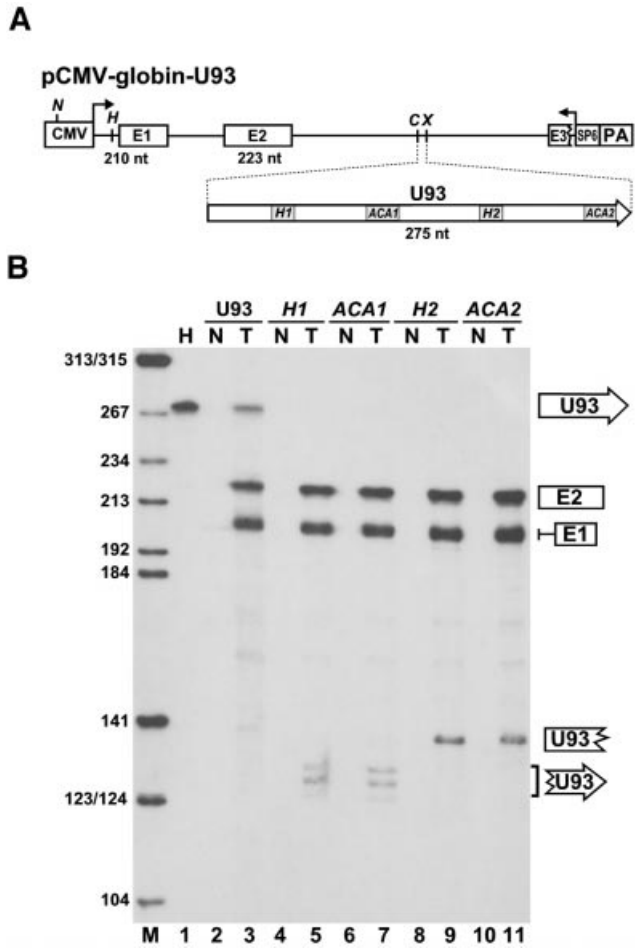

Figure 4. Transient expression of human U93 RNA in COS-7 cells. (**A**) Schematic representation of the pCMV-globin expression construct. The CMV promoter, full-length (E1 and E2) and partial (E3) exons of the human β-globin gene, the SP6 RNA polymerase promoter (SP6) and the polyadenylation region of the bovine growth hormone gene (PA) are indicated. Relevant restriction sites are shown (*N*, *Nde*I; *H*, *Hin*dIII; *C*, *Cla*I; and *X*, *Xho*I). Open arrow indicates the coding region of human U93 RNA. In the U93-*H1*, U93-*ACA1*, U93-*H2* and U93-*ACA2* constructs, the indicated box element was replaced for a stretch of C residues. (**B**) RNase A/T1 protection analysis. Plasmids used for transfection of COS-7 cells and specific probes utilised for mappings are indicated at the top. Lanes N and T represent mapping reactions with RNAs obtained from non-transfected and transfected cells, respectively. Lane H, mapping of HeLa cellular RNAs. RNA fragments protected by the first and second exons of the spliced β-globin mRNA, the U93 RNA and the 5′- and 3′-terminal portions of the U93 RNA are indicated on the right. Lane M, size marker in nucleotides.

We noticed that the first and third hairpins of U93 are followed by potential box H sequences (63-AAAGCA-68 and 202-AGAGAA-207) and that the second and the last hairpins are followed by potential box ACA motifs (134-AUA-136 and 270-ACA-272). This strongly suggested that the human U93 RNA is composed of two tandemly arranged box H/ACA RNA domains.

Northern analysis of mouse, rat, cow and carp nuclear RNAs performed with a human U93-specific antisense RNA probe revealed hybridising RNAs of the size of human U93 (data not shown). The full-length sequences of the mouse and cow U93 RNAs were obtained by RT–PCR followed by 5′- and 3′-end RACE experiments (see Materials and Methods). A comparison of the sequences and two-dimensional structures of the human, mouse and cow U93 RNAs is shown in Figure 2. Strikingly, most of the evolutionarily variable nucleotides are located in predicted single-stranded regions, namely in the three hinge and the 3′-terminal tail regions as well as in internal and terminal loop structures. Contrary to the fact that the hinge regions show the highest sequence variability,

nucleotides in the putative H1, H2, ACA1 and ACA2 motifs are perfectly conserved in the human, mouse and cow U93 RNAs, pointing to the functional importance of these sequences. In most cases, altered nucleotides located in double-stranded regions do not interfere with the formation of perfect double helices (see positions U7, A107, A164, A165, A196, G184, G232, A254). Even more tellingly, transition of the A168 residue to a G residue in the cow U93 RNA is restored by a U to C compensatory base change in the opposite strand of the proposed double helix. Taken together, these observations strongly supported the correctness of the proposed secondary structure of U93 and confirmed the conclusion that the mammalian U93 RNA is composed of two box H/ACA snoRNA-like domains.

The human U93 RNA specifically accumulates in Cajal bodies

Mammalian box H/ACA RNAs accumulate either in the nucleolus or in the nucleoplasmic Cajal bodies (8,18). Upon fractionation of human HeLa cells, the U93 RNA and the U4 spliceosomal snRNA were found mainly in the nucleoplasmic fraction, while the U19 box H/ACA and the U3 box C/D authentic snoRNAs co-purified with the nucleolar fraction (Fig. 3B). To determine the precise nucleoplasmic localisation of U93, we used *in situ* fluorescent microscopy (Fig. 3C). Probing of HeLa cells with a U93-specific fluorescent antisense RNA probe revealed that the U93 RNA localises to sharp dot-like structures in the nucleoplasm. Staining the same cells with an antibody directed against p80 coilin, a molecular marker of Cajal bodies (35), demonstrated that the U93 RNA perfectly co-localises with p80 coilin. Likewise, upon transient overexpression of the human U93 RNA in HeLa cells (for details, see below), the overproduced U93 RNA showed a specific co-localisation with p80 coilin. Thus far, all box C/D and box H/ACA RNAs residing in Cajal bodies have been implicated in post-transcriptional modification of pol II-specific spliceosomal snRNAs (8,11,18). Indeed, we noticed that sequences in the internal loop of the 3′-terminal hairpin of U93 are capable of positioning the U54 residue in the U2 snRNA for pseudouridylation (Fig. 3D). We concluded that (i) the U93 box H/ACA-H/ACA composite RNA represents a new member of scaRNAs and (ii) the U93 scaRNA likely functions in pseudouridylation of the RNA pol II-specific U2 spliceosomal snRNA.

Elements essential for accumulation of the U93 box H/ACA-H/ACA scaRNA

The box H and ACA elements play a crucial role in accumulation of yeast and mammalian box H/ACA snoRNAs (14,15). Since the U93 RNA possesses two putative box H (H1 and H2) and ACA (ACA1 and ACA2) elements, we have tested the functional importance of each of these elements in RNA accumulation. The genomic copy of the human U93 RNA is located in an intron of a series of reported spliced expressed sequence tags, indicating that the U93 RNA is generated by intron processing (36,37). Therefore, to express the human U93 RNA, its coding region was inserted into the second intron of the human β-globin gene controlled by the cytomegalovirus (CMV) promoter (Fig. 4A). The resulting pCMV-globin-U93 expression construct was transfected into simian COS-7 cells and expression of the U93 RNA was tested by RNase A/T1 mapping using a sequence-specific antisense RNA probe (Fig. 4B, lane 3). As compared with the authentic human U93 RNA (lane 1), the plasmid-born U93 RNA was faithfully processed from the globin pre-mRNA, further supporting the notion that U93 is indeed an intron-encoded RNA.

When either the box H1, ACA1, H2 or ACA2 motif of the U93 gene was replaced with a C stretch of appropriate length in the pCMV-globin-U93 construct, accumulation of the full-length U93 RNA was completely abolished in transfected COS-7 cells, although the globin host mRNA was correctly expressed in each case (Fig. 4B, lanes 5, 7, 9 and 11). Upon disruption of the box H1 or ACA1 motif, RNase mapping resulted in accumulation of a protected RNA doublet with a molecular size that corresponds to the predicted length of the processed 3′-terminal box H/ACA domain of the U93 RNA (~130 nt) (Fig. 4B, lanes 5 and 7). On the other hand, alteration of the H2 or ACA2 motif resulted in the accumulation of an RNA of the expected size (~140 nt) of the 5′-terminal H/ACA domain of U93 (Fig. 4B, lanes 9 and 11). Indeed, the identity of these RNAs was confirmed by RNase mappings performed with probes specific for either the 5′- or the 3′-terminal half of the U93 RNA (data not shown). These results demonstrated that both the 5′- and the 3′-terminal box H/ACA RNA domains of the human U93 RNA can independently accumulate. However, mapping of HeLa cellular RNA failed to detect any accumulating fragment of the U93 RNA (Fig. 4B, lane 1, and data not shown), indicating that normally neither the 5′- nor the 3′-terminal box H/ACA domain of U93 is expressed separately.

We next investigated whether the 5′- and 3′-terminal domains of the U93 RNA, when they are expressed independently, still accumulate in Cajal bodies. Mouse cells transfected with the pCMV-globin expression construct carrying the U93, U93-*H1* or U93-*H2* genes were probed with fluorescent antisense probes specific for the 5′- and 3′-terminal domains of the U93 RNA (Fig. 5). The Cajal bodies of the transfected mouse cells were visualised by co-expression of the coilin-Dsred2 fluorescent recombinant protein. Similar to the full-length human U93 RNA, both the 5′- and 3′-terminal box H/ACA domains of the RNA accumulated in Cajal bodies. This demonstrates that both box H/ACA domains of U93 possess functionally active localisation signals which can direct the Cajal body-specific accumulation of the two domains independently of one another.

DISCUSSION

Site-specific synthesis of 2′-*O*-methylated nucleotides and pseudouridines in rRNAs and spliceosomal snRNAs is directed by guide RNAs which can be classified into three structurally and functionally well defined families (Fig. 1). The box C/D RNAs direct 2′-*O*-methylation and the box H/ACA RNAs guide pseudouridylation of rRNAs and snRNAs. Another minor group of composite box C/D-H/ACA RNAs function both in 2′-*O*-methylation and pseudouridylation of snRNAs (18,27). In this study, we have identified and characterised a novel type of pseudouridylation guide RNA. The U93 RNA is composed of two tandemly arranged box H/ACA RNA domains and, therefore, it carries two box H and ACA motifs. This unique architecture of the

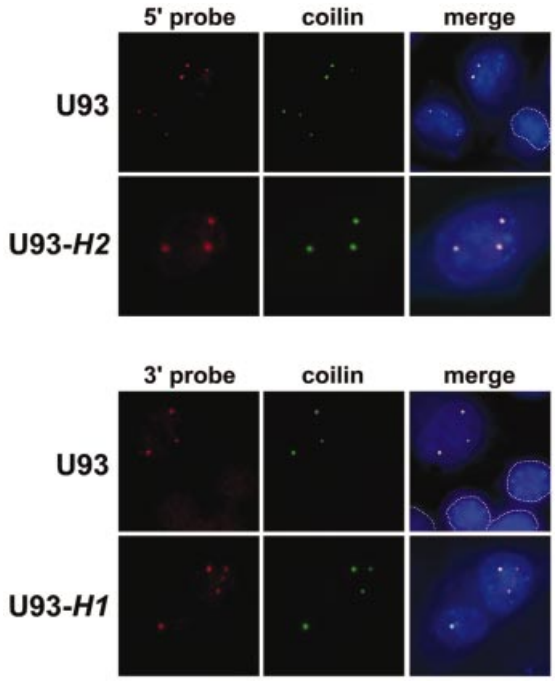

Figure 5. *In situ* localisation of the 5′- and 3′-terminal box H/ACA domains of human U93 expressed in mouse cells. Mouse L929 cells were transfected with the pCMV-globin-U93, pCMV-globin-U93*H1* and pCMV-globin-U93*H2* expression constructs (see Fig. 4A). The transiently expressed U93 RNA was visualised by a fluorescent oligonucleotide or an antisense RNA probe specific for the 5′- and 3′-terminal domain of the human U93 RNA, respectively. Cajal bodies of mouse cells were detected by co-expression of the coilin-Dsred2 fluorescent protein. For other details, see the legend to Figure 3C.

U93 RNA is conserved at least in human, mouse and cow (Fig. 2).

Previous characterisation of the human U85 box C/D-H/ACA composite RNA showed that the unusual structural organisation of this class of modification guide RNAs could be explained by several facts. Alteration of the 5′-terminal C or the 3′-terminal D box of the U85 RNA completely abolished the expression of both the full-length U85 RNA and box H/ACA domain of the RNA (27). This indicated that accumulation of the human U85 box C/D-H/ACA RNA is supported exclusively by its box C/D domain and that the box H/ACA domain of the RNA lacks metabolic stability. In the case of the newly discovered U93 box H/ACA-H/ACA composite RNA, all conserved box elements (H1, ACA1, H2 and ACA2) are required for accumulation of the full-length RNA. However, accumulation of the 5′- and 3′-terminal box H/ACA domains of U93 is not interdependent. In other words, both box H/ACA domains of the U93 RNA possess all those elements which are essential for accumulation (Fig. 4).

Thus far, all 2′-*O*-methylation and pseudouridylation guide RNAs implicated in modification of the RNA pol II-specific U1, U2, U4 and U5 spliceosomal snRNAs have been found to reside in the nucleoplasmic Cajal bodies (18). It seems that these guide RNAs possess specific *cis*-acting targeting elements which are responsible for the their Cajal body specific localisation. Currently, we have found that the Cajal body-specific localisation signals of the human U85 C/D-H/ACA scaRNA are located in the box H/ACA domain of the RNA and that the box C/D domain of U85 alone cannot localise to Cajal bodies (P.Richard, X.Darzacq, C.Verheggen, E.Bertrand and T.Kiss, manuscript in preparation). The human U93 box H/ACA-H/ACA RNA also accumulates in Cajal bodies and, unexpectedly, both box H/ACA domains of the U93 RNA possess functionally active Cajal body-specific targeting elements (Fig. 5). So, in contrast to the U85 box C/D-H/ACA RNA, the unusual structural organisation of the U93 box H/ACA-H/ACA RNA cannot be explained by the metabolic instability or incorrect intracellular trafficking of the two domains of the RNA.

The box C/D and H/ACA domains of the U85 RNA function in 2′-*O*-methylation and pseudouridylation of two neighbouring nucleotides in the U5 spliceosomal snRNA. This suggests that co-expression of guide RNAs directing modification of the same substrate RNA is advantageous for the cell (27). The putative pseudouridylation pocket in the 3′-terminal hairpin of the U93 RNA is predicted to direct pseudouridylation of the U2 spliceosomal snRNA at position U54 (Fig. 3D). Since both the 5′- and 3′-terminal hairpins of box H/ACA RNAs can carry functional pseudouridylation pockets (23,38), the four hairpins of the U93 box H/ACA-H/ACA RNA, in principle, could direct pseudouridylation of four different substrate uridines. It seems, however, unlikely that the first and third hairpins of U93 contain functional pseudouridylation pockets, since several evolutionarily altered nucleotides are present in these regions (Fig. 2). On the contrary, the second hairpin carries a conserved internal loop that possesses the characteristic topology of a functional pseudouridylation pocket. This putative pseudouridylation pocket of U93 lacks complementarity to rRNAs, spliceosomal snRNAs or any known stable RNAs, including tRNAs. Therefore, it seems likely that the second hairpin of the U93 RNA directs pseudouridylation of a not yet identified RNA. Whether this putative target RNA of U83, like all substrate RNAs of Cajal body-specific guide RNAs, has a cellular function related to pre-mRNA splicing remains an intriguing speculation.

In summary, identification of the U93 RNA that is composed of two box H/ACA RNA domains further supports the idea that snRNA structural domains are frequently used to build novel composite RNAs. In addition to the recently characterised box C/D-H/ACA scaRNAs (18,27), the vertebrate and yeast telomerase RNAs carry a box H/ACA and Sm domain, respectively (39,40). In principle, acquisition of a structurally and functionally well defined snRNA domain may contribute to metabolic stability, may direct intracellular trafficking or may provide a new cellular function for the newly made composite RNA.

ACKNOWLEDGEMENTS

We are indebted to Y. de Preval for synthesis of oligonucleotides. A.M.K. was funded by the French Government and the Hungarian Academy of Sciences. B.E.J. is a recipient of a long term EMBO fellowship. X.D. and C.V. were funded by la Fondation pour la Recherche Médicale and Association pour la Recherche contre le Cancer, respectively. Our work was supported by grants from Association pour la Recherche

contre le Cancer, la Ligue Nationale contre le Cancer, the French MNRT (ACI) and the Hungarian Research Foundation (OTKA, T29042 and T31738).

REFERENCES

1. Yu,Y.T., Scharl,E.C., Smith,C.M. and Steitz,J.A. (1999) The growing world of small nuclear ribonucleoproteins. In Gesteland,R.F. Cech,T.R. and Atkins,J.F. (eds), *The RNA World*. Cold Spring Harbor Laboratory Press, Cold Spring Harbor, New York, pp. 487–524.
2. Maxwell,E.S. and Fournier,M.J. (1995) The small nucleolar RNAs. *Annu. Rev. Biochem.*, **64**, 897–934.
3. Nguyen,V.T., Kiss,T., Michels,A.A. and Bensaude,O. (2001) 7SK small nuclear RNA binds to and inhibits the activity of CDK9/cyclin T complexes. *Nature*, **414**, 322–325.
4. Yang,Z., Zhu,Q., Luo,K. and Zhou,Q. (2001) The 7SK small nuclear RNA inhibits the CDK9/cyclin T1 kinase to control transcription. *Nature*, **414**, 317–322.
5. Blackburn,E. (1999) Telomerase. In Gesteland,R.F, Cech,T.R. and Atkins,J.F. (eds.), *The RNA World*. Cold Spring Harbor Laboratory Press, Cold Spring Harbor, New York, pp. 609–635.
6. Smith,C.M. and Steitz,J.A. (1997) Sno storm in the nucleolus: new roles for myriad small RNPs. *Cell*, **89**, 669–672.
7. Bachellerie,J.P., Cavaillé,J. and Qu,L.H. (2000) Nucleotide modifications of eukaryotic rRNAs: the world of small nucleolar RNAs revisited. In Garrett,R.A., Douthwaite,S.R., Matheson,A.T., Moore,P.B. and Noller,H.F. (eds), *The Ribosome: Structure, Function, Antibiotics and Cellular Interactions.* ASM Press, Washington, pp. 191–203.
8. Kiss,T. (2001) Small nucleolar RNA-guided post-transcriptional modification of cellular RNAs. *EMBO J.*, **20**, 3617–3622.
9. Filipowicz,W. and Pogacic,V. (2002) Biogenesis of small nucleolar ribonucleoproteins. *Curr. Opin. Cell Biol.*, **14**, 319–327.
10. Terns,M.P. and Terns,R.M. (2002) Small nucleolar RNAs: versatile *trans*-acting molecules of ancient evolutionary origin. *Gene Expr.*, **10**, 17–39.
11. Kiss,T. (2002) Small nucleolar RNAs: an abundant group of noncoding RNAs with diverse cellular functions. *Cell*, **109**, 145–148.
12. Tycowski,K.T., Shu,M.D. and Steitz,J.A. (1996) A mammalian gene with introns instead of exons generating stable RNA products. *Nature*, **379**, 464–466.
13. Kiss-László,Z., Henry,Y. and Kiss,T. (1998) Sequence and structural elements of methylation guide snoRNAs essential for site-specific ribose methylation of pre-rRNA. *EMBO J.*, **17**, 797–807.
14. Balakin,A.G., Smith,L. and Fournier,M.J. (1996) The RNA world of the nucleolus: two major families of small RNAs defined by different box elements with related functions. *Cell*, **86**, 823–834.
15. Ganot,P., Caizergues-Ferrer,M. and Kiss,T. (1997) The family of box ACA small nucleolar RNAs is defined by an evolutionarily conserved secondary structure and ubiquitous sequence elements essential for RNA accumulation. *Genes Dev.*, **11**, 941–956.
16. Omer,A.D., Ziesche,S., Ebhardt,H. and Dennis,P.P. (2002) In vitro reconstitution and activity of a C/D box methylation guide ribonucleoprotein complex. *Proc. Natl Acad. Sci. USA*, **99**, 5289–5294.
17. Hoang,C. and Ferre-D'Amare,A.R. (2001) Cocrystal structure of a tRNA Psi55 pseudouridine synthase: nucleotide flipping by an RNA-modifying enzyme. *Cell*, **107**, 929–939.
18. Darzacq,X., Jády,B.E., Verheggen,C., Kiss,A.M., Bertrand,E. and Kiss,T. (2002) Cajal body-specific small nuclear RNAs: a novel class of 2′-*O*-methylation and pseudouridylation guide RNAs. *EMBO J.*, **21**, 2746–2756.
19. Kiss-László,Z., Henry,Y., Bachellerie,J.P., Caizergues-Ferrer,M. and Kiss,T. (1996) Site-specific ribose methylation of preribosomal RNA: a novel function for small nucleolar RNAs. *Cell*, **85**, 1077–1088.
20. Cavaillé,J., Nicoloso,M. and Bachellerie,J.P. (1996) Targeted ribose methylation of RNA *in vivo* directed by tailored antisense RNA guides. *Nature*, **383**, 732–735.
21. Tycowski,K.T., Smith,C.M., Shu,M.D. and Steitz,J.A. (1996) A small nucleolar RNA requirement for site-specific ribose methylation of rRNA in *Xenopus*. *Proc. Natl Acad. Sci. USA*, **93**, 14480–14485.
22. Ni,J., Tien,A.L. and Fournier,M.J. (1997) Small nucleolar RNAs direct site-specific synthesis of pseudouridine in ribosomal RNA. *Cell*, **89**, 565–573.
23. Ganot,P., Bortolin,M.L. and Kiss,T. (1997) Site-specific pseudouridine formation in preribosomal RNA is guided by small nucleolar RNAs. *Cell*, **89**, 799–809.
24. Tycowski,K.T., You,Z.H., Graham,P.J. and Steitz,J.A. (1998) Modification of U6 spliceosomal RNA is guided by other small RNAs. *Mol. Cell*, **2**, 629–638.
25. Ganot,P., Jády,B.E., Bortolin,M.L., Darzacq,X. and Kiss,T. (1999) Nucleolar factors direct the 2′-*O*-ribose methylation and pseudouridylation of U6 spliceosomal RNA. *Mol. Cell. Biol.*, **19**, 6906–6917.
26. Lange,T.S. and Gerbi,S.A. (2000) Transient nucleolar localization Of U6 small nuclear RNA in *Xenopus laevis* oocytes. *Mol. Biol. Cell*, **11**, 2419–2428.
27. Jády,B.E. and Kiss,T. (2001) A small nucleolar guide RNA functions both in 2′-*O*-ribose methylation and pseudouridylation of the U5 spliceosomal RNA. *EMBO J.*, **20**, 541–551.
28. Sambrook,J., Fritsch,E.F. and Maniatis,T. (1989) *Molecular Cloning: A Laboratory Manual*. Cold Spring Harbor Laboratory Press, Cold Spring Harbor, New York.
29. Kiss,T. and Filipowicz,W. (1993) Small nucleolar RNAs encoded by introns of the human cell cycle regulatory gene RCC1. *EMBO J.*, **12**, 2913–2920.
30. Datta,A.K. (1995) Efficient amplification using 'megaprimer' by asymmetric polymerase chain reaction. *Nucleic Acids Res.*, **23**, 4530–4531.
31. Boulon,S., Basyuk,E., Blanchard,J.M., Bertrand,E. and Verheggen,C. (2002) Intra-nuclear trafficking: insight from live cell imaging. *Biochimie*, in press.
32. Tyc,K. and Steitz,J.A. (1989) U3, U8 and U13 comprise a new class of mammalian snRNPs localized in the cell nucleolus. *EMBO J.*, **8**, 3113–3119.
33. Goodall,G.J., Wiebauer,K. and Filipowicz,W. (1990) Analysis of pre-mRNA processing in transfected plant protoplasts. In Dahlberg,J.E. and Abelson,J.N. (eds), *Methods in Enzymology*, Academic Press, New York, Vol. 181, pp. 148–161.
34. Zuker,M., Mathews,D.H. and Turner,D.H. (1999) Algorithms and thermodynamics for RNA secondary structure prediction: A practical guide. In Barciszewski,J. and Clark,B.F.C. (eds), *RNA Biochemistry and Biotechnology*. Kluwer Academic Publishers, Dordrecht, The Netherlands, pp. 11–43.
35. Andrade,L.E., Chan,E.K., Raska,I., Peebles,C.L., Roos,G. and Tan,E.M. (1991) Human autoantibody to a novel protein of the nuclear coiled body: immunological characterization and cDNA cloning of p80-coilin. *J. Exp. Med.*, **173**, 1407–1419.
36. Tollervey,D. and Kiss,T. (1997) Function and synthesis of small nucleolar RNAs. *Curr. Opin. Cell Biol.*, **9**, 337–342.
37. Weinstein,L.B. and Steitz,J.A. (1999) Guided tours: from precursor snoRNA to functional snoRNP. *Curr. Opin. Cell Biol.*, **11**, 378–384.
38. Bortolin,M.L., Ganot,P. and Kiss,T. (1999) Elements essential for accumulation and function of small nucleolar RNAs directing site-specific pseudouridylation of ribosomal RNAs. *EMBO J.*, **18**, 457–469.
39. Seto,A.G., Zaug,A.J., Sobel,S.G., Wolin,S.L. and Cech,T.R. (1999) *Saccharomyces cerevisiae* telomerase is an Sm small nuclear ribonucleoprotein particle. *Nature*, **401**, 177–180.
40. Mitchell,J.R., Cheng,J. and Collins,K. (1999) A box H/ACA small nucleolar RNA-like domain at the human telomerase RNA 3′ end. *Mol. Cell. Biol.*, **19**, 567–576.